Ethanol detection and monitoring using Surface Acoustic Wave Sensor

Rishikesh Srinivasaraghavan Govindarajan[1, a], Mackenzie Tobin[2, b], Zefu Ren[1, a], Michael Ricciardella[1, a], Foram Madiyar[1, *c], Daewon Kim[1, *a]
[a]Dept. of Aerospace Engineering; [b]Dept. of Biomedical Engineering; [c]Dept. of Physical Science;
[1]Embry-Riddle Aeronautical University, 1 Aerospace Blvd., Daytona Beach, FL, USA 32114
[2]Virginia Commonwealth University, 907 Floyd Ave, Richmond, VA, USA 23284

ABSTRACT

Surface acoustic wave (SAW) sensors are a promising microelectromechanical systems (MEMS) technology for gas detection due to their high sensitivity, stability, and rapid response. This study presents the development of a room-temperature SAW sensor for ethanol detection, a critical VOC. The sensor incorporates ZnO particles, fabricated via the electrospray deposition technique, as the sensing layer on a flexible polymer substrate and utilizes 3D printed two-port electrode configurations. Real-time experiments demonstrate a linear relationship between ethanol concentration (0~500 ppm) and resonant frequency shift, with a sensitivity of 0.407 ± 0.008 kHz/ppm. The sensor, in its default state, detects mechanical strain through frequency shifts, while the incorporation of a sensing layer extends its functionality to gas detection, highlighting its multifunctional potential for aerospace environmental monitoring and safety applications.

Keywords: ethanol detection, SAW sensor, sensing layer, multifunctional

1. INTRODUCTION

The increasing demand for multifunctional sensors has driven significant advancements in microelectromechanical systems (MEMS)-based technologies, particularly in aerospace, biomedical and environmental monitoring applications[1-3]. Effective real-time monitoring of environmental and structural parameters such as gas concentrations and mechanical strains is essential for ensuring safety and operational efficiency. However, conventional sensing approaches often require separate devices for different measurements, increasing system complexity, power consumption, and integration challenges. Surface acoustic wave (SAW) sensors, a leading MEMS technology, have emerged as a promising platform for multifunctional sensing due to their high sensitivity, rapid response time and stable operation[4-6]. By integrating multiple sensing capabilities within a single device, SAW-based systems offer a compact, scalable and energy-efficient solution for real-time monitoring applications.

Aerospace applications, particularly in space exploration, present a unique set of challenges where environmental and structural health monitoring (SHM) is essential. Long-duration space missions require continuous assessment of air quality and material integrity to ensure crew safety and mission sustainability. Ethanol, a prominent volatile organic compound (VOC), constitutes a significant fraction of chemical contamination in spacecraft atmospheres, often representing over 70% of total alcohol concentration inside the International Space Station (ISS)[7]. Ethanol levels in confined space environments can result from metabolic processes, off-gassing of onboard materials, or contamination from operational sources. Effective real-time monitoring of ethanol levels is therefore crucial for maintaining a safe and controlled environment[8].

The performance of SAW-based ethanol sensors depends heavily on the choice of the sensing layer. Zinc oxide (ZnO) is widely recognized as a sensing material for detecting gases like carbon dioxide (CO_2), ammonia (NH_3), ethanol (C_2H_5OH), and nitrogen dioxide (NO_2) due to its high surface reactivity, long-term stability, and rapid response[9-12]. However, the performance of ZnO-based sensors is strongly influenced by the deposition technique used to fabricate the sensing layer. Conventional methods including spray pyrolysis, spin coating and vapor deposition have been extensively explored, yet

* kimd3c@erau.edu; phone 1-386-226-7262; madiyarf@erau.edu; phone 1-386-226-6673

Nondestructive Characterization and Monitoring of Advanced Materials, Aerospace, Civil Infrastructure, and Transportation XIX, edited by Tzuyang Yu, Andrew L. Gyekenyesi, Peter J. Shull, H. Felix Wu, Proc. of SPIE Vol. 13436, 134360D · © 2025 SPIE · 0277-786X · doi: 10.1117/12.3051529

each presents limitation. Spray pyrolysis required high temperatures that will degrade polymer-based substrates, while spin coating struggles with achieving uniform film thickness, especially on non-planar surfaces[13, 14]. Although vapor deposition techniques yield high-quality films, they involve complex procedures and costly equipment, limiting their accessibility for scalable applications[15, 16].

Electrospray deposition has emerged as a promising alternative, offering precise control over morphology and uniform coating while operating at room temperature. This method eliminates thermal damage concerns, facilitates uniform coating on complex geometries, and offers a scalable, cost-effective solution for sensor fabrication. By optimizing electrospray parameters, the surface characteristics of the ZnO layer can be tailored to enhance gas adsorption efficiency, thereby improving the ethanol detection sensitivity.

This study presents the development of a SAW-based sensor that integrates ethanol gas sensing with mechanical strain measurement capabilities to operate at the room temperature. Polyvinylidene Fluoride (PVDF), a well-known polymer for its excellent piezoelectric properties, is selected as a substrate material due to its compliance to flexible micro-MEMS device fabrication. The sensor utilized ZnO particles as the sensing layer, leveraging ZnO's high surface area, and chemical stability to enhance ethanol detection sensitivity. By leveraging scalable fabrication techniques, including electrospray deposition for ZnO sensing layer and 3D printed electrode configurations, this research aims to offer versatile, cost-effective solutions for real-time monitoring in both aerospace and biomedical multifunctional sensing systems.

2. DEVELOPMENT OF SAW DEVICE WITH SENSING LAYER

The fabrication of the gas sensor involves precise steps, beginning with the deposition of a ZnO particles on a PVDF substrate using the electrospray technique, followed by the printing of fine electrode pattern, as shown in Figure 1.

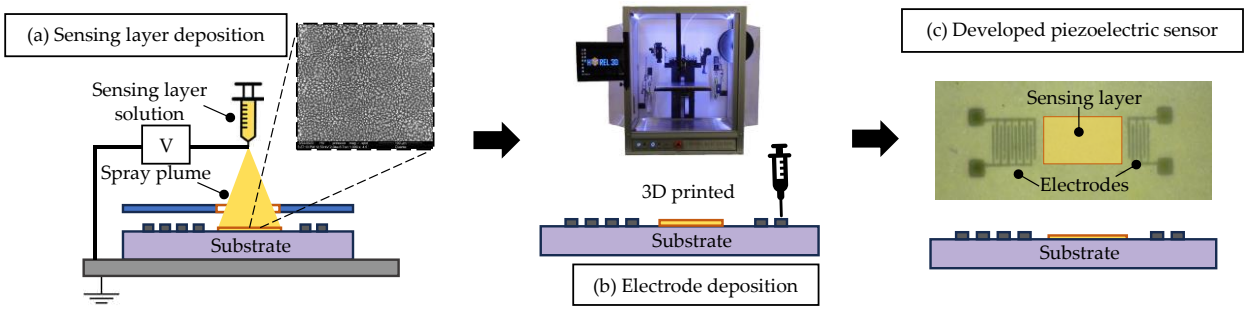

Figure 1. Schematic of wave-based sensor development: (a) sensing layer deposition using electrospray process, (b) electrode deposition using 3D printing method and (c) complete sensor device for gas detection.

2.1 ZnO particles deposition via Electrospray

Electrospray deposition is used to deposit ZnO particles onto the PVDF substrate. In this process, a high voltage is applied to a liquid passing through a capillary nozzle, generating an electrostatic force that overcomes the liquid's surface tension and forms a Taylor cone[17], as shown in Figure 2 (a). When the threshold voltage is reached, a fine jet of liquid is ejected from the cone's apex, breaking into smaller droplets due to Coulombic repulsion[18]. This mechanism enables the controlled deposition of particles onto the substrate.

Several operational parameters, including flow rate, applied voltage, exposure time and solution properties, must be carefully controlled to mitigate potential issues such as clogging, inconsistent spray patterns, and non-uniform deposition. In this study, a confined spraying area was defined using a masking tape to ensure the ZnO particles deposition only on the designated region of the PVDF substrate. The electrospray process exhibits predictable patterns: increasing the applied voltage extends the length of the stable jet while narrowing the spray angle, whereas a higher flow rate results in a longer jet with a reduced spray angle[19, 20]. To optimize the deposition conditions, key parameters – flow rate, applied voltage, and exposure time were systematically varied through parametric sweeps. After each deposition cycle, the distribution of ZnO particles was evaluated using optical microscopy to ensure uniformity and complete coverage of the substrate. The

optimized electrospray parameters were determined to be a voltage range of 8-10 kV, a flow rate of 0.012 mL/min, and a needle to substrate distance of 85 mm. Each sample underwent three electrospray cycles, each consisting of 1 min of deposition followed by 3 min of drying. These parameters ensured uniform deposition and effective adhesion of ZnO particles to the PVDF substrate, as shown in Figure 2 (b). Furthermore, the hydrophilicity of the PVDF substrate was enhanced prior to the particle deposition via air plasma treatment. This treatment introduces polar functional groups onto the polymer surface, increasing its surface energy and improving wettability. Contact angle measurements, shown in Figure 2 (c) and (d), revealed a decrease from 73.8° (untreated) to 50.13° (treated), confirming enhanced hydrophilicity. This modification played a crucial role in improving the particle adhesion, thereby enabling uniform deposition of ZnO layer during the electrospray process.

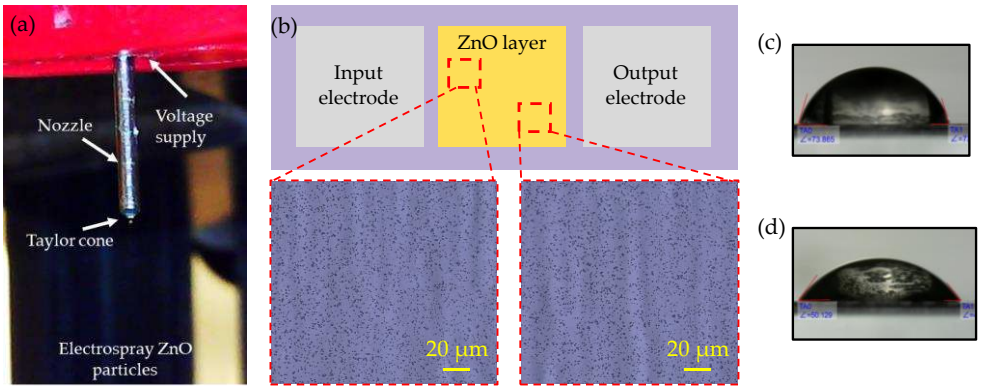

Figure 2. (a) Optical image illustrating the ZnO electrospray setup, (b) microscope images of sensing layer with deposited ZnO particles and contact angle measurements of water on polymer substrate (c) before and (d) after air plasma.

In addition to optimizing substrate wettability, maintaining a stable Taylor cone throughout the electrospray process requires continuous adjustment of the applied voltage within the specified range. Variations in the surrounding electrostatic environment, such as interference from external sources or the absence of a controlled enclosure, can affect spray stability. Furthermore, the formation of a thin conductive layer after each deposition cycle altered the local electrostatic field, necessitating real-time voltage adjustments to maintain a stable and efficient electrospray deposition.

2.2 Morphological and elemental analysis

SEM images of the ZnO deposited PVDF substrate (Figure 3 (a)) reveal a uniform distribution of ZnO particles, with an average particle size of ~0.6 µm observed through particle size distribution analysis (Figure 3 (b)) over a selected area of 58.7 µm × 55.1 µm and based on 826 particles, demonstrating the effectiveness of the optimized electrospray process.

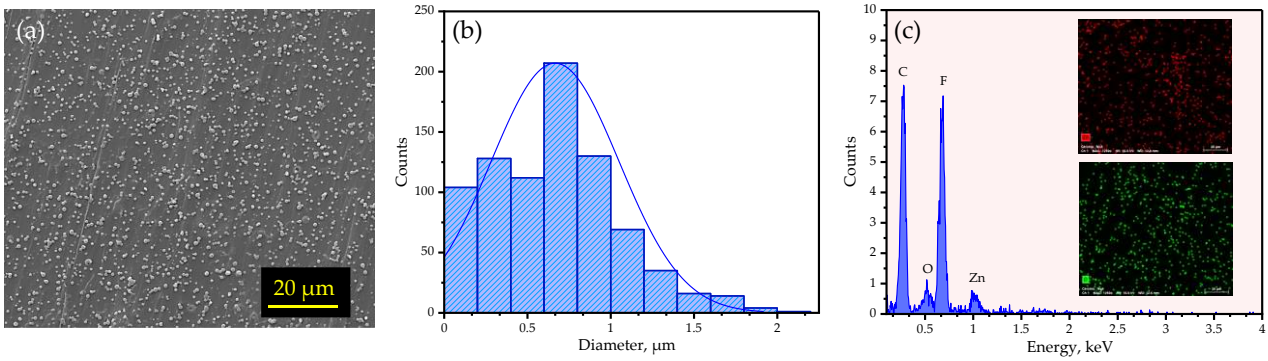

Figure 3. (a) SEM image of deposited ZnO particles, (b) ZnO particle distribution, and (c) EDX spectra with elemental content of ZnO particles deposited on PVDF substrate. The inset shows distribution of Zn and O distribution.

The particles are well dispersed, indicating consistent deposition across the substrate. Elemental analysis through EDX (Figure 3 (c)) shows prominent peaks of zinc (Zn) and oxygen (O), confirming the presence of ZnO on the substrate. Additionally, the strong peaks for carbon (C) and fluorine (F) correspond to the PVDF substrate, validating the successful deposition of ZnO onto the surface. These observations highlight the effectiveness of the optimized electrospray process in achieving homogenous ZnO deposition.

2.3 3D printed electrode deposition

Following the deposition of the ZnO sensing layer, the interdigital transducer (IDT) electrodes are fabricated using a HYREL 3D printer. Conductive silver paste is dispensed through a syringe setup fitted with a Gauge 34 needle (outer diameter: 0.2 mm, inner diameter: 0.08 mm) to create the electrode pattern. Key printing parameters, such as the print speed of 2.6 mm/sec and precise X-Y motion control, are governed by G-code inputs to the printer. After optimization, IDT electrode patterns with a nominal width of 150 µm are successfully printed, exhibiting continuous lines and secure adhesion to both the base substrate and around the deposited sensing layer, as shown in Figure 4.

During the deposition process, the formation of small silver paste islands was observed, particularly at the corners and edge of the printed IDT patterns. Additionally, a secondary layer of conductive material was deposited due to the bidirectional motion of the printer, where the printhead retracted the same path in the reverse direction. This effect is attributed to the buildup of pressure on the syringe needle, which leads to the deposition of an excessive amount of conductive material, resulting in a thicker electrode layer than originally intended. Despite these minor inconsistencies, the electrodes exhibited strong adhesion to the base substrate without significant impact on the functionality of the electrodes. The optimized electrospray and 3D printing parameters enable reliable ethanol detection, while the selection of sensing layer material can be customized to target specific gases, providing flexibility for detecting a range of VOCs and broadening the sensor's application potential.

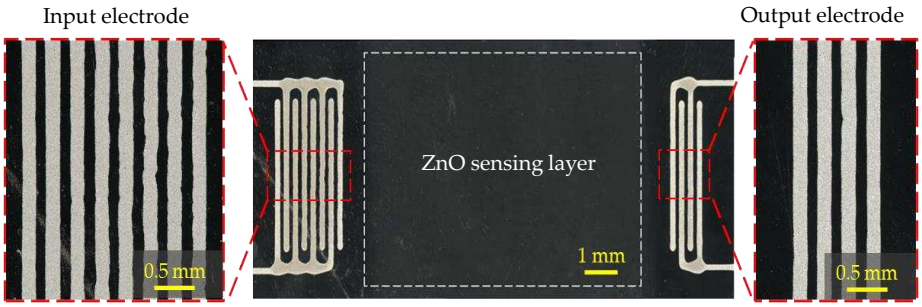

Figure 4. Microscope images of 3D printed input and output electrodes with deposited ZnO sensing layer.

3. GAS SENSING CHARACTERISTICS AND PERFORMANCE EVALUATION

3.1 Ethanol detection under controlled concentration gradients

For the ethanol detection experiments, a custom gas chamber setup was employed, designed to facilitate precise monitoring of the sensor's response to varying gas concentrations. This setup includes provisions for connecting RF probes, enabling simultaneous data collection while controlling the gas supply. A mass flow regulator is connected to a cylinder containing ethanol gas, with split valve used to control the gas flow. Additionally, a vacuum pump is integrated into the system to ensure an airtight seal and prevent gas leakage over time, as illustrated in Figure 5. The sensor's performance was evaluated by monitoring changes in resonant frequency upon exposure to ethanol gas. These measurements are vital for assessing the sensor's sensitivity. The Bode VNA 100, with its S-parameter (S_{11} and S_{21}) data, was used to track the sensor's response across different ethanol concentrations, providing valuable insights into the sensor's behavior.

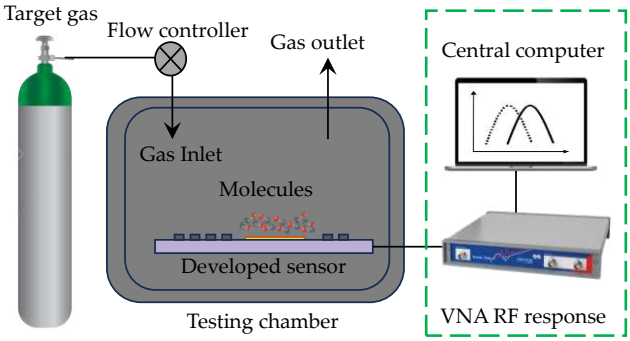

Figure 5. Schematic illustration of the gas sensing test system, consisting of test chamber with a sensor mounted inside. The inset depicts the data collection and processing devices, which provides useful real-time gas detection information.

As shown in Figure 6, the representative harmonic resonant frequency response of the sensor was recorded under no-gas and gas-in conditions. The introduction of ethanol gas, with a maximum concentration of 515 ± 17 ppm and a constant flow rate of 0.3 L/min, resulted in a notable frequency shift and a corresponding change in peak intensity due to the mass loading effect.

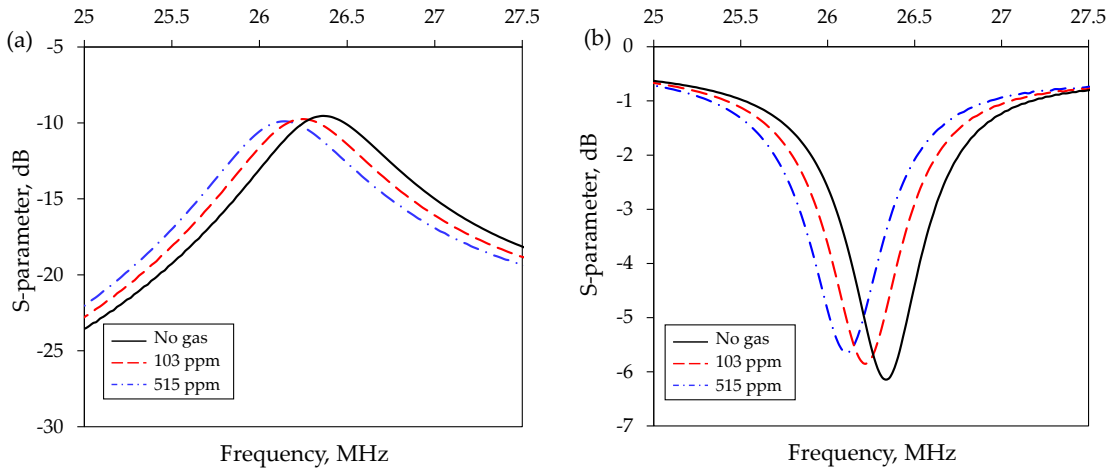

Figure 6. Experimental resonant frequency response of the developed gas sensor with varying gas concentrations (a) S_{21} and (b) S_{11}.

3.2 Sensitivity characterization and Limit of detection estimation

The sensor exhibits an average sensitivity of 0.407 kHz/ppm to ethanol vapor, as shown Figure 7, demonstrating its capability to detect ethanol concentration variations with high accuracy and stability. The limit of detection (LOD) for ethanol is determined to be 16.7 ppm using the three-sigma method[21], which considers the sensors' baseline noise and achieved sensitivity. The achieved LOD indicates the sensor's capability to detect ethanol at low concentrations highlighting its reliability and suitability for applications requiring precise VOC monitoring.

The fabricated sensor exhibits up to 10% variation in the resonant peak across sensor samples, attributed to inherent accuracy limitations of both IDT and sensing layer fabrication. While primarily designed for ethanol detection, the sensor also responds to mechanical strain, with strain-induced frequency shifts occurring within MHz range[22]. The recovery time for strain-induced shifts is significantly shorter compared to gas-induced shifts, as ethanol adsorption delays peak restoration. These findings underscore the sensor's multifunctionality in both gas detection and strain monitoring, with potential for further methodological studies to differentiate these effects.

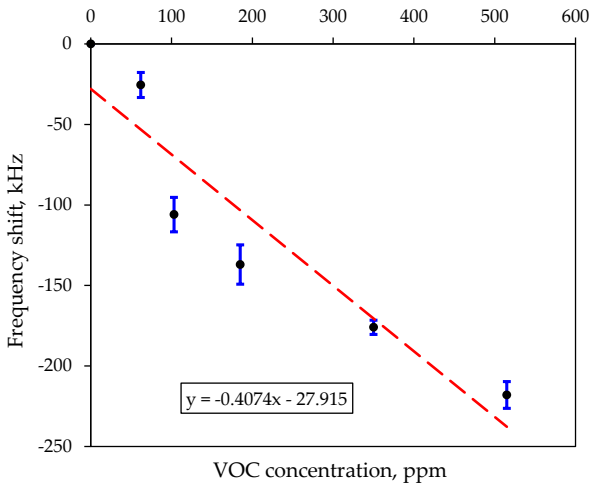

Figure 7. The sensitivity evaluation of the developed gas sensor towards ethanol detection.

4. CONCLUSION

In summary, a room-temperature SAW sensor integrating ZnO particles as the sensing layer via electrospray deposition and 3D printed IDTs is successfully developed for ethanol detection. The sensor demonstrates a linear frequency response to ethanol (VOC) up to 515 ± 17 ppm, achieving a sensitivity of 0.407 ± 0.008 kHz/ppm and a LOD of 16.7 ppm. Beyond gas sensing, its inherent ability to measure mechanical strain underscores its multifunctionality. Future work will focus on optimizing the sensing layer design, including incorporation of microstructures to enhance sensitivity, as well as refining methodologies to differentiate gas and mechanical strain induced shifts. These advancements will further improve measurement accuracy and expand the sensor's applicability in aerospace environmental monitoring and safety applications.

ACKNOWLEDGMENT

This material is based upon work supported in part by the National Science Foundation under Grant No. 2050887, 2347094, 2229155 and National Aeronautics & Space Administration through the University of Central Florida's NASA Florida Space Grant (FSGC). The opinions, findings, and conclusions or recommendations expressed are those of the author(s) and do not necessarily reflect the views of the National Science Foundation or NASA FSGC.

REFERENCES

[1] Okuda, S., Ono, T., Kanai, Y., Ikuta, T., Shimatani, M., Ogawa, S., Maehashi, K., Inoue, K., and Matsumoto, K., "Graphene Surface Acoustic Wave Sensor for Simultaneous Detection of Charge and Mass," *ACS Sensors,* **3**(1), 200-204 (2018). https://doi.org/10.1021/acssensors.7b00851

[2] Wang, H., Liang, X., Zhang, J., Zhang, L., Xie, H., Zhao, Z., and Tan, Q., "A wireless demodulation system based on a multi-parameter resonant sensor," *Review of Scientific Instruments,* **94**(3), (2023). https://doi.org/10.1063/5.0141478

[3] Yang, Y., Mengue, P., Mishra, H., Floer, C., Hage-Ali, S., Petit-Watelot, S., Lacour, D., Hehn, M., Han, T., and Elmazria, O., "Wireless Multifunctional Surface Acoustic Wave Sensor for Magnetic Field and Temperature Monitoring," *Advanced Materials Technologies,* **7**(3), 2100860 (2022). https://doi.org/https://doi.org/10.1002/admt.202100860

[4] Liang, X., Zhang, L., Tan, Q., Cheng, W., Hu, D., Li, S., Jing, L., and Xiong, J., "Temperature, pressure, and humidity SAW sensor based on coplanar integrated LGS," *Microsystems & Nanoengineering,* **9**(1), 110 (2023). https://doi.org/10.1038/s41378-023-00586-0

[5] Mishra, H., Hehn, M., Hage-Ali, S., Petit-Watelot, S., Mengue, P. W., Zghoon, S., M'Jahed, H., Lacour, D., and Elmazria, O., "Microstructured Multilayered Surface-Acoustic-Wave Device for Multifunctional Sensing," *Physical Review Applied,* **14**(1), 014053 (2020). https://doi.org/10.1103/PhysRevApplied.14.014053
[6] Srinivasaraghavan Govindarajan, R., Rojas-Nastrucci, E., and Kim, D., "Surface Acoustic Wave-Based Flexible Piezocomposite Strain Sensor," *Crystals,* **11**(12), 1576 (2021). https://doi.org/https://doi.org/10.3390/cryst11121576
[7] Perry, J., Carter, L., Kayatin, M., Gazda, D., McCoy, T., and Limero, T., "Assessment of Ethanol Trends on the ISS," *International Conference on Environmental Systems* (2016).
[8] Elias Abi-Ramia Silva, T., Burisch, F., and Güntner, A. T., "Gas sensing for space: Health and environmental monitoring," *TrAC Trends in Analytical Chemistry,* **177**, 117790 (2024). https://doi.org/https://doi.org/10.1016/j.trac.2024.117790
[9] Ding, J., Chen, S., Han, N., Shi, Y., Hu, P., Li, H., and Wang, J., "Aerosol assisted chemical vapour deposition of nanostructured ZnO thin films for NO2 and ethanol monitoring," *Ceramics International,* **46**(10), 15152-15158 (2020). https://doi.org/https://doi.org/10.1016/j.ceramint.2020.03.051
[10] Hasan, M. N., Maity, S., Sarkar, A., Bhunia, C. T., Acharjee, D., and Joseph, A. M., "Simulation and fabrication of SAW-based gas sensor with modified surface state of active layer and electrode orientation for enhanced H2 gas sensing," *Journal of Electronic Materials,* **46**(2), 679 (2017). https://doi.org/https://doi.org/10.1007/s11664-016-5128-7
[11] Kang, Y., Yu, F., Zhang, L., Wang, W., Chen, L., and Li, Y., "Review of ZnO-based nanomaterials in gas sensors," *Solid State Ionics,* **360**, 115544 (2021). https://doi.org/https://doi.org/10.1016/j.ssi.2020.115544
[12] Waikar, M. R., Raste, P. M., Sonker, R. K., Gupta, V., Tomar, M., Shirsat, M. D., and Sonkawade, R. G., "Enhancement in NH3 sensing performance of ZnO thin-film via gamma-irradiation," *Journal of Alloys and Compounds,* **830**, 154641 (2020). https://doi.org/https://doi.org/10.1016/j.jallcom.2020.154641
[13] Alvarado, J. A., Maldonado, A., Juarez, H., and Pacio, M., "Synthesis of Colloidal ZnO Nanoparticles and Deposit of Thin Films by Spin Coating Technique," *Journal of Nanomaterials,* **2013**, 903191 (2013). https://doi.org/https://doi.org/10.1155/2013/903191
[14] Lee, S. D., Nam, S.-H., Kim, M.-H., and Boo, J.-H., "Synthesis and Photocatalytic Property of ZnO nanoparticles Prepared by Spray-Pyrolysis Method," *Physics Procedia,* **32**, 320-326 (2012). https://doi.org/https://doi.org/10.1016/j.phpro.2012.03.563
[15] Guan, Y. F., and Pedraza, A. J., "Synthesis and alignment of Zn and ZnO nanoparticles by laser-assisted chemical vapor deposition," *Nanotechnology,* **19**(4), 045609 (2008). https://doi.org/https://doi.org/10.1088/0957-4484/19/04/045609
[16] Mohammed, R., Ahmed, S., Abdulrahman, A., and Hamad, S., "Synthesis and Characterizations of ZnO Thin Films Grown by Physical Vapor Deposition Technique," *Journal of Applied Science and Technology Trends,* **1**(2), 135 - 139 (2020). https://doi.org/10.38094/jastt1456
[17] Fernández de la Mora, J., "The Fluid Dynamics of Taylor Cones," *Annual Review of Fluid Mechanics,* **39**(Volume 39, 2007), 217-243 (2007). https://doi.org/https://doi.org/10.1146/annurev.fluid.39.050905.110159
[18] Rohner, T. C., Lion, N., and Girault, H. H., "Electrochemical and theoretical aspects of electrospray ionisation," *Physical Chemistry Chemical Physics,* **6**(12), 3056-3068 (2004). https://doi.org/https://doi.org/10.1039/B316836K
[19] Li, W., Lin, J., Wang, X., Jiang, J., Guo, S., and Zheng, G., [Electrospray Deposition of ZnO Thin Films and Its Application to Gas Sensors], (2018). https://doi.org/https://doi.org/10.3390/mi9020066
[20] Marinov, G., Lovchinov, K., Madjarova, V., Strijkova, V., Vasileva, M., Malinowski, N., and Babeva, T., "Aluminum-doped zinc oxide thin films deposited by electrospray method," *Optical Materials,* **89**, 390-395 (2019). https://doi.org/https://doi.org/10.1016/j.optmat.2019.01.055
[21] Şengül, Ü., "Comparing determination methods of detection and quantification limits for aflatoxin analysis in hazelnut," *Journal of Food and Drug Analysis,* **24**(1), 56-62 (2016). https://doi.org/https://doi.org/10.1016/j.jfda.2015.04.009
[22] Srinivasaraghavan Govindarajan, R., Madiyar, F., and Kim, D., "Flexible Piezoelectric Wave-Based Sensor: Numerical Analysis And Validation." https://doi.org/10.1115/SMASIS2022-91069